Proceedings of 8th International Conference on Mechanical Engineering and Renewable Energy 2025
10-12 December, 2025, Chattogram, BANGLADESH

SciEn Conference Series: Engineering Vol. 4, 2026, pp 29-34 https://doi.org/10.38032/scse.2026.4.21

Design and Development of a Low-Cost Phototransistor-Based Pyranometer for Solar Resource Assessment

Ishtiak Mohammad Zia[1], Md. Siam Hossain[1] , Shanawas sakrio[1] , Professor Dr. Mazharul Islam[1]*

[1]Department of Mechanical Engineering, Ahsanullah University of Science & Technology, Dhaka-1208, Bangladesh

ABSTRACT

Pyranometer is a device used to measure solar irradiance that reaches the Earth. It is commonly utilized in solar energy systems, agricultural research, and weather monitoring. The high cost of conventional pyranometers, particularly in developing nations, can prevent their widespread usage. This thesis presents a low-cost phototransistor-based pyranometer that is simple to manufacture using readily available components. The low-cost pyranometer design presented in this thesis provides an affordable and accessible alternative to traditional pyranometers. When light hits the phototransistor, a small electrical voltage is generated. A NodeMCU development board is used to measure the solar irradiance from this voltage by using the conversion factor of calibration of the pyranometer. The performance of the pyranometer was assessed by evaluating real-time data, and the results were analyzed through graphical representation and mathematical calculations. Calibration of the pyranometer was done by using the CM 11 pyranometer, which can be considered a standard device in the process of calibrating pyranometers. The simple design and low price of this pyranometer make it an excellent tool for education and performing experiments, particularly in developing countries like Bangladesh, where the price of conventional pyranometers is expensive.

Keywords: Solar Resource Assessment, Pyranometer, Renewable Energy, Phototransistor, Calibration.

1. Introduction

A pyranometer is a type of sensor used to measure the solar irradiance received by a surface. This measurement is crucial in several industries, including meteorology, agriculture, and renewable energy. The first pyranometer was developed by Moll-Gorczynski in 1893, and since then, it has undergone several modifications to improve its accuracy and performance [1]. For many years, solar irradiance has been measured by various sensors defined and classified by the ISO:9060 standard [2]. The most widely used type of pyranometer uses thermal sensors with a black absorber surface for receiving radiation in the solar spectrum (the main wavelength is 300-3000 nm) [3]. For a pyranometer, it is important to obtain accurate irradiance at any incident angle, considering the incident angle of sunlight that changes with time. A phototransistor-based pyranometer that measures both the quantity and intensity of solar irradiance was designed and developed for this research. In addition, an Internet of Things (IoT) based microcontroller unit (MCU) or development board is used to create a prototype with IoT applications. It has low-power CPUs that can run a variety of programming languages. Using the ThingSpeak IoT platform, this device collects data from sensors and transfers it to a local server or a server on the internet (cloud server) [4]. This makes it possible for the pyranometer to be readily programmed to carry out several tasks and incorporated into a larger system, such as a weather station. Moreover, the pyranometer's data may be processed by a NodeMCU and displayed in a variety of ways, including on an LCD screen or a computer. The majority of pyranometers measure solar irradiance using photovoltaic cells, phototransistors, or other light-sensing elements that produce a modest electrical current or voltage in response to incoming solar irradiance. Then, this electrical current is read, processed, and converted into solar irradiance measurements using microcontrollers for solar strength and intensity estimation. Even though these sensors offer high sensitivity in their measurements, commercially available pyranometers are associated with expensive acquisition and maintenance costs [5]. It is therefore necessary to develop a solar pyranometer that is economical, reliable, and can be used in a wide range of situations. A phototransistor is used to function as a sensitive light component in a phototransistor-based pyranometer, which measures solar irradiance. Since the phototransistor established a lower cost per unit and improved response in terms of sensitivity, it was chosen as the sensor element for solar irradiance measurement [6]. The NodeMCU is the system's main processing brain. To begin, the primary voltage must be supplied by the battery for the microcontroller to function. The system will then be turned on and ready to use. The newly developed instrument uses a phototransistor as its sensing element, allowing it to detect and measure the intensity of incident sunlight. Solar irradiance is detected by the phototransistor and converted into an electrical voltage signal. A change in the phototransistor's conductivity of electricity causes a change in the phototransistor's output voltage. The magnitude of the voltage change is related to the intensity of incoming solar radiation. The phototransistor-based pyranometer successfully transforms incident solar radiation into an electrical output, which then can be adjusted to produce meaningful solar irradiance measurements. This signal is processed by the NodeMCU, and the data is sent to a cloud server via the Internet of Things (IoT) network. The buck converter assures a steady supply of power from the battery. It is capable of measuring both direct and diffuse solar

*Corresponding Author Email Address: mohammad.ishtiakzia@gmail.com

irradiance combined i.e. global solar irradiance. Data acquisition systems used frequently record and process the phototransistor's electrical output. The components were carefully selected through a literature review, considering factors like spectral response, angular response, and the temperature effect. The technical specifications of the components used in this research match the ISO:9060 guidelines. The spectral sensitivity was a flat response within a 5% spectral range of 0.3 to 3 microns. The experimental setup was done in the same location to maintain the cosine response and directional response. The operating temperatures of the components matched the temperature of the system. That's why it was observed that the temperature response was within 2% in the case of any change up to 20℃. The calibration process was done by comparing the results with Global Solar Atlas data and a trustworthy pyranometer named CM 11, which maintains these ISO standards itself. One of the criteria of the ISO:9060 standard was that the output should be in W/m^2. The measured value of solar irradiance from the pyranometer is shown on a digital display in W/m^2, as well as the voltage and temperature.

2. Materials & Methods

2.1 Methodology

The research was conducted by following a simple yet effective methodology, which starts from choosing the components to analyze the data of the finished product. An extensive literature review was conducted to select the components carefully and to meet the ISO:9060 standards. A market survey was done to ensure that the components are locally available and affordable. After collecting the components and creating the final design, all the parts were assembled carefully. The data were taken periodically to observe any deviation. The data acquisition system was designed to monitor solar irradiance and analyze the trends and variations. Cross-validation was done by using a trustworthy, accurate pyranometer named CM 11. The methodology is strictly followed to ensure standard fabrication, better calibration, and accurate data collection. Mathematical and Graphical analyses were done properly. Fig. 1 shows the methodology below.

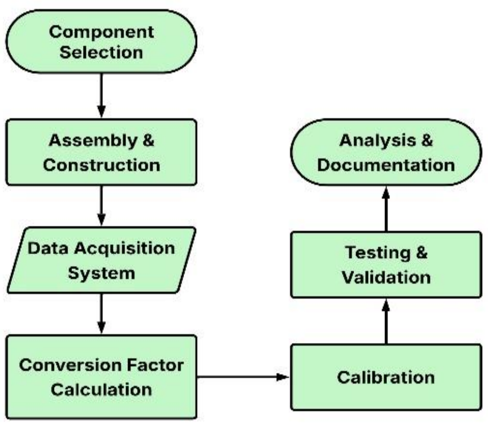

Fig. 1: Flowchart of design & experiment methodology

The conversion technology is based on a phototransistor, which converts solar energy into electrical energy (volts).

2.2 Components

Table 1 shows the detailed list of components to build the phototransistor-based pyranometer.

Table 1: List of equipment used

Equipment List	Unit	Cost (BDT)
Phototransistor -ST-1KLA	1	80
LCD Display	1	380
Lithium Polymer Battery (7.4 V)	1	300
Node MCU-ESP8266	1	530
Buck Converter	1	90
Temperature Sensor DHT 11	1	165
Casing	1	1960
Resistor (10KΩ)	1	5
Total	8	3510

3. Design & Assembly

Fig. 2 shows the detailed block diagram of the whole system of the phototransistor-based pyranometer.

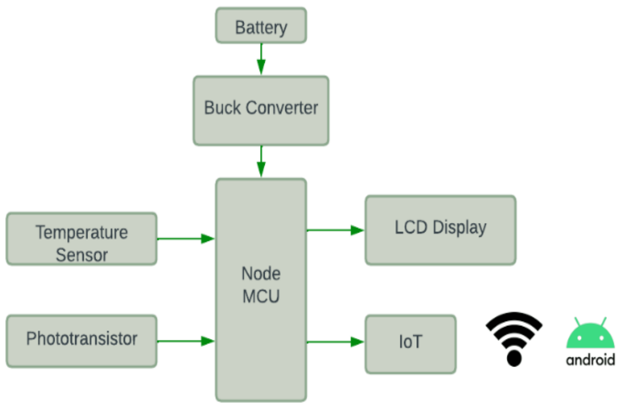

Fig. 2: Block diagram of phototransistor-based pyranometer

Fig. 3 illustrates the internal circuit diagram of the phototransistor-based pyranometer.

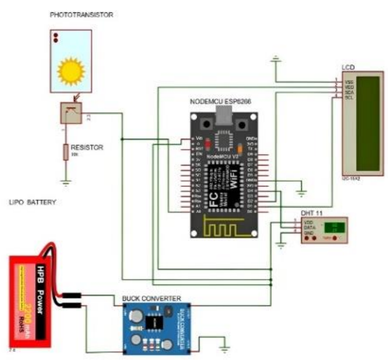

Fig. 3: Circuit diagram of phototransistor-based pyranometer

The phototransistor-based pyranometer's final casing design for this research is shown in Fig. 4. An additional layer of material is added to the lower, slanted side of the box to further improve the design. This additional layer aids in strengthening the bond between the structure and the glass frame. The design is unique since it allows for the removal of the glass top portion of the box. This was done on purpose to make it simple to examine and repair any internal components, such as the circuit components, in the event of necessity.

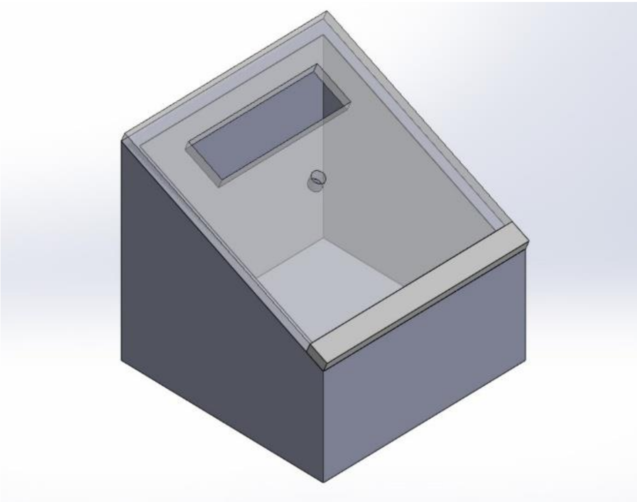

Fig. 4: The final design of the phototransistor-based pyranometer's casing

The casing of the pyranometer is set at a specific angle of 23 degrees, which corresponds exactly to the latitude of Dhaka, Bangladesh. A 3D printer was used to fabricate this case. Fig. 5 shows the developed pyranometer. A distinguishing feature of this design lies in the upper part of the pyranometer's casing, which is constructed from transparent glass. This glass lid was seamlessly fused to the rest of the casing by combining a strip of PVC sheet and specialized adhesive.

Fig. 5: Fabricated model of a phototransistor-based pyranometer

4. Calibration & Conversion Factor

Calibration was done to enhance the accuracy. This is why preliminary data were collected from 12:00 to 1:00 at noon, listed in Table 2. The phototransistor-based pyranometer gives an output in millivolts. A commercially proven pyranometer known as CM 11 was used to measure the real-time accurate solar irradiance. CM 11 Pyranometer had a conversion factor of 8.38×10^{-6} V/W/m^{2,} which was used to convert its voltage to solar irradiance. From that accurate solar irradiance, a conversion factor was formulated for the phototransistor-based pyranometer to convert the output voltage to solar irradiance. After the Pyranometer was calibrated, it was used to take real-time data for later on.

Table 2: Sample data collection before calibration

Time	Phototransistor based pyranometer output (mV)	CM 11 pyranometer output (mV)	Solar irradiance measured by CM 11 pyranometer (W/m^2)
12:00	360.30	6.4	763.72
12:05	402.61	6.9	825.35
12:10	353.71	6.5	778.16
12:15	260.61	4.6	547.28
12:20	251.50	4.4	523.12
12:25	266.00	4.8	571.90
12:30	359.70	6.3	762.56
12:35	290.30	5.1	609.63
12:40	218.74	3.7	437.48
12:45	349.45	6.1	733.84
12:50	338.30	5.8	696.89
12:55	332.45	5.8	694.82
1:00	340.71	6.0	722.30

After fabricating the pyranometer, calibration processes were followed to make the results more accurate and precise. Pyranometers should have a conversion factor as pyranometers work based on conversion technology. As the phototransistor measures mainly the output voltage (V_o) when exposed to sunlight, a calculation was done to convert the voltage to solar irradiance ($E_{\downarrow,Solar}$) comparing the results with a known commercially proven pyranometer CM 11 [7]. For the CM 11 pyranometer, manufacturers provided a conversion factor that is 8.38×10^{-6} V/W/m^2. From Table 2, at 12:00 pm, CM 11 output was 6.4 mV. For that, solar irradiance was found to be 763.72 W/m^2. At the same time, the phototransistor-based pyranometer's output was 360.3 mV. Equation (1) shows the conversion factor (S),

$$S=\frac{V_o}{E_{\downarrow,Solar}}=\frac{360.3\times10^{-3}}{763.72}=4.72\times10^{-4}\ \text{V/W/m}^2 \qquad (1)$$

This same calculation was done for all data, and an average conversion factor was found to be 4.7×10^{-4} V/W/m^2. And, the following Eq. (2) can be used to get the solar irradiance value for the phototransistor-based pyranometer. Maximum sensor output was found to be 402.61 mV. Equation (2) shows the solar irradiance measured by the phototransistor-based pyranometer,

$$E_{\downarrow,Solar}=\frac{V_o}{S}=\frac{402.61\times10^{-3}}{4.7\times10^{-4}}=856.61\ \text{W/m}^2 \qquad (2)$$

5. Result & Discussion

Table 3 shows the data for solar irradiance vs time measured by the Phototransistor-based pyranometer at a location with geographical coordinates (23.772543°, 90.404574°) from 8:00 in the morning to 13:00 at noon at a regular interval of 5 minutes. Due to bad weather, it was not possible to take the data for a whole day.

Table 3: Irradiance measurements by the phototransistor-based pyranometer

Time	Irradiance (W/m^2)	Time	Irradiance (W/m^2)
08:00	225.75	09:25	384.82
08:05	242.13	09:30	316.05
08:10	273.63	09:35	343.77
08:15	251.47	09:40	346.92
08:20	279.09	09:45	382.83
08:25	266.84	09:50	416.64
08:30	389.02	09:55	406.35
08:35	358.26	10:00	415.59
08:40	330.33	10:05	412.44
08:45	289.48	10:10	366.24
08:50	286.23	10:15	376.53
08:55	285.18	10:20	449.50
09:00	313.00	10:25	458.74
09:05	321.19	10:30	476.07
09:10	322.24	10:35	469.98
09:15	332.53	10:40	568.47
10:50	618.76	12:00	715.05
10:55	651.42	12:05	725.23
11:00	645.54	12:10	777.00
11:05	548.1	12:15	757.05
11:10	556.5	12:20	767.13
11:15	581.91	12:25	715.05
11:20	594.72	12:30	882.84
11:25	588.21	12:35	886.09
11:30	601.23	12:40	724.18
11:35	599.34	12:45	709.27
11:40	672.00	12:50	737.73
11:45	678.93	12:55	749.07
11:50	533.08	13:00	740.83
11:55	517.12	-	-

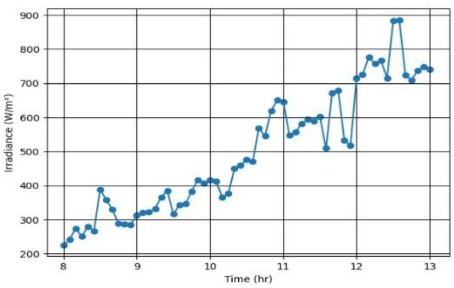

Fig. 6: Irradiance vs time measured by phototransistor-based pyranometer

From Fig. 6, it can be seen that the solar irradiance was increasing as the day went on. The maximum solar irradiance was found to be 886.09 W/m^2 at 12:35, which makes sense as it is nearly the solar noon. After that, it started decreasing as the day went on. The minimum solar irradiance was 225.75 W/m^2 at 8:00 in the morning.

5.1 Comparative Analysis

To prove the accuracy of the phototransistor-based pyranometer, a graph was plotted comparing the data of the CM 11 reference pyranometer and phototransistor based pyranometer at the same time. CM 11 pyranometer was used as a reference pyranometer to validate the measurement data of the phototransistor-based pyranometer, as CM 11 pyranometer is a trustworthy and accurate device. The location and time were the same for both pyranometers to maintain the standards of experimental setup, such as temperature and humidity. Both the pyranometers had zero offset values. Pyranometers were calibrated before taking the measurements. The comparison gives an overall clear idea of the authenticity of the phototransistor-based pyranometer. The collected comparative data by the phototransistor-based pyranometer and the CM 11 pyranometer from 12:00 to 2:00 at noon is shown in Table 4.

Table 4: Irradiance Comparison for the Pyranometers

Time	Solar irradiance measured by CM 11 pyranometer (W/m^2)	Solar irradiance measured by phototransistor-based pyranometer (W/m^2)
12:00	763.72	726.50
12:05	799.52	758.80
12:10	811.45	771.30
12:15	680.19	646.00
12:20	262.52	250.00
12:25	214.79	202.50
12:30	322.19	301.00
12:35	751.78	715.15
12:40	608.59	580.50
12:45	179.00	168.05
12:50	715.99	680.10
12:55	739.85	705.60
1:00	775.65	746.86
1:05	799.52	760.60
1:10	763.72	724.50
1:15	202.82	191.67
1:20	178.99	172.30
1:25	250.59	238.06
1:30	274.46	261.70
1:35	286.39	273.10
1:40	298.32	283.40
1:45	322.19	306.10
1:50	334.12	375.50
1:55	346.06	329.60
2:00	357.99	340.09

Fig.7 shows the comparative graph between the reference pyranometer CM 11 and the phototransistor-based pyranometer from 12:00 to 2:00 at noon. It can be seen from the graph that the two curves almost match each other, giving an idea that the accuracy of the developed Phototransistor-based pyranometer is very high and satisfactory. The abrupt decline in the irradiance values depicted in the graph can be attributed to the prevailing weather conditions, specifically the sudden appearance of clouds and fluctuations in sunlight during that period.

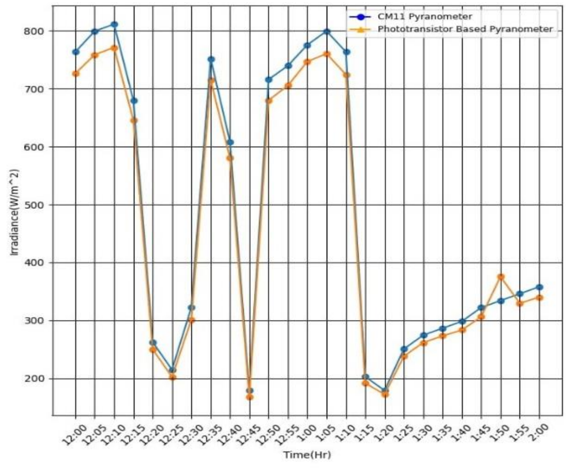

Fig. 7: Data comparison graph

5.2 Correlation Analysis

Fig. 8 shows the linear correlation between the reference pyranometer CM 11 and the phototransistor-based pyranometer.

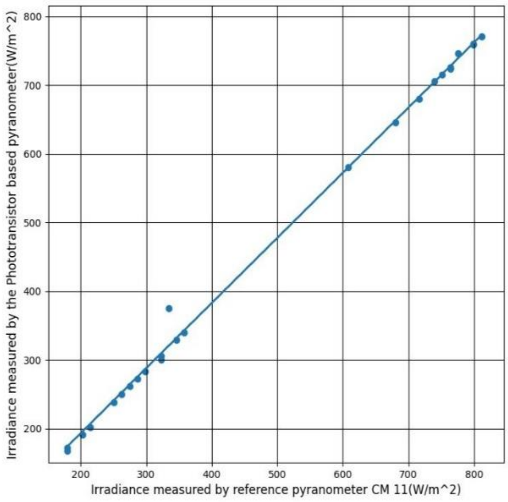

Fig. 8: Correlation analysis between pyranometers; Pearson and Spearman's coefficient

Pearson's correlation coefficient in Eq. (3),

$$r_p = \frac{\sum (x_i - \bar{x})(y_i - \bar{y})}{\sqrt{\sum (x_i - \bar{x})^2 \sum (y_i - \bar{y})^2}} \tag{3}$$

Here, x_i is the individual value of irradiance measured by the CM 11 pyranometer and $\bar{x}$ is the mean value of irradiances measured by the CM 11 pyranometer, which is 481.6 W/m^2.Again, y_i is the individual value of irradiance measured by the phototransistor based pyranometer and $\bar{y}$ is the mean value of irradiances measured by it, which is 460.4 W/m^2 in Table 4.

Pearson's Correlation Coefficient: 0.998.

Spearman's correlation Coefficient in Eq. (4),

$$r_s = 1 - \frac{6 \sum d_i^2}{n(n^2-1)} \tag{4}$$

n is the number of cases, which is 25, and d is the difference in ranks in the two pyranometers' measured irradiances in Table 4.

Spearman's Rank Correlation Coefficient: 0.996

Pearson's correlation and Spearman's rank correlation coefficients indicate the strength and direction of a linear relationship between the two variables. The correlation values are nearly 1. So the null hypothesis can be rejected, and it can be established that the relation between these two pyranometers is strongly positive and linear. It can be expected to observe a linear increase or decrease in the readings of these two pyranometers [8] [9].

5.3 The Uncertainty Analysis

Two simple formulas, as written in Eq. (5) and in Eq. (6), available in statistics, are often used to calculate the standard deviation and uncertainty due to random error in the sample [10].

$$\sigma = \sqrt{\frac{1}{n-1}\sum_{i=1}^{n}(x_i - \bar{x})^2} \tag{5}$$

$$\sigma_{\bar{X}} = \frac{\sigma}{\sqrt{n}} \tag{6}$$

where σ is the standard deviation, n is the sample size, x_i is the sample values, $\bar{x}$ is the sample mean, and $\sigma_{\bar{X}}$ is the standard error of the mean of the phototransistor-based pyranometer's data in Table 4.

Sample mean ($\bar{x}$) = 460.4 W/m^2, Sample size (n)= 25, Standard deviation (σ) = 234.1 W/m^2, Standard error of mean ($\sigma_{\bar{x}}$) = 46.82 W/m^2

The value of the measurement for the phototransistor-based pyranometer is 460.4 W/m^2 with uncertainty of ± 46.82 W/m^{2,} which is satisfactory considering the fact that these data are highly weather dependent.

Uncertainty analysis shows a nearly 10.17% error in the Pyranometer, favorable for design requirements, indicating high accuracy.

6. Conclusion

The present work studied the research gaps in the field of solar resource assessment using pyranometers. Designing an affordable and accurate pyranometer was the primary goal of this research. An extensive literature review was conducted, and the final design was developed for the pyranometer. Calibration was done to achieve more accuracy as well as regular, trustworthy measurements with minimal cost. The pyranometer was developed using the NodeMCU microcontroller and a phototransistor. A detailed experiment was done to take the readings of the pyranometer. Highly sensitive and expensive, a commercial pyranometer named CM 11 was used as a reference pyranometer to test the accuracy of the phototransistor-based pyranometer and validate it. Then the results were compared by plotting graphs using Python. The graphs were mainly based on irradiance over time for the developed pyranometer as well as the data taken by the reference pyranometer, CM 11. After that, correlation and uncertainty analyses were done. Finally, a comparison graph was plotted in which the irradiances measured by the phototransistor-based pyranometer and the CM 11 pyranometer were shown over time. This graph played a crucial role in this research to prove that the phototransistor-based pyranometer is affordable yet highly accurate. Overall, the accuracy was nearly 90%, which is satisfactory for this range of cost. The pyranometer was successfully developed and has the potential to meet the requirements of local researchers affordably.

7. References

[1] K. Behrens, "Radiation sensors," *Springer Handbook of Atmospheric Measurements,* pp. 297-357, 2021.

[2] International Organization for Standardization, "*ISO 9060:2018-Solar energy-specification and classification of instruments for measuring hemispherical solar and direct solar radiation*," Nov.2018.[Online].Available:https://cdn.standards.iteh.ai/samples/67464/8a4f719696624455b8bb2b071e5389d6/ISO-9060-2018.pdf. [Accessed: Aug. 11, 2025].

[3] Y.A. Eltbaakh, M. Ruslan, M. Alghoul, M. Othman, K. Sopian, and M. Fadhel. "Measurement of total and spectral solar irradiance: Overview of existing research," *Renewable and Sustainable Energy Reviews,* vol. 15, no. 3, pp. 1403-1426, 2011.

[4] Y.S. Parihar, "Internet of things and nodemcu," *journal of emerging technologies and innovative research,* vol. 6, no. 6, p. 1085, 2019.

[5] R. C. d. Barros, J.M.S. Callegari, D. d. C. Mendonca, W.C.S. Amorim, M.P. Silva and H.A Pereira, "Low-cost solar irradiance meter using ldr sensors," in *IEEE International Conference on Industry Applications (INDUSCON)*, 2018.

[6] S. Roy, S.C. Panja and S.N. Patra, "An embedded system to measure ground-based solar irradiance signal," *Measurement,* vol. 173, pp. 108-598, 2021.

[7] Kipp & Zonen B.V., "*CM 11 Pyranometer CM 14 Albedometer Manual, Kipp & Zonen, Delft, The Netherlands,2000*." 2000. [Online]. Available: https://www.kippzonen.com/Download/48/CM-11-Pyranometer-CM-14-Albedometer-Manual. [Accessed : Aug. 4, 2025].

[8] Obilor, E. Issac & Amadi. and Eric, "Test for significance of Pearson's correlation coefficient", *International Journal of Innovative Mathematics, Statistics & Energy Policies*, vol. 6, no. 1, 2018.

[9] Z. Jerrold, "Spearman Rank Correlation," *Encycle Biostat,* vol. 5, p. {}, 2005.

[10] H.Castrup,"Distributions for uncertainty analysis," in *International Dimensional Workshop*, 2001.

7. Nomenclature

Symbol	Meaning	Unit
$E_{\downarrow,Solar}$	Solar irradiance	W/m^2
T	Temperature	℃
t	Time	s
V_o	Output voltage	V
R	Resistance	Ω
S	Conversion factor/Sensitivity	V/W/m^2
r_p	Pearson's Correlation Coefficient	Dimensionless
r_s	Spearman's Rank Correlation Coefficient	Dimensionless
σ	Standard deviation	W/m^2
$\sigma_{\bar{X}}$	Standard error of mean	W/m^2